

Health condition assessment for vegetation exposed to heavy metal pollution through airborne hyperspectral data

Bikram Pratap Banerjee · Simit Raval · Hao Zhai · Patrick Joseph Cullen

Received: 20 March 2017 / Accepted: 26 October 2017 / Published online: 3 November 2017
© Springer International Publishing AG, part of Springer Nature 2017

Abstract Recent advancements in hyperspectral remote sensing technology now provide improved diagnostic capabilities to assess vegetation health conditions. This paper uses a set of 13 vegetation health indices related to chlorophyll, xanthophyll, blue/green/red ratio and structure from airborne hyperspectral reflectance data collected around a derelict mining area in Yerranderie, New South Wales, Australia. The studied area has ten historic mine shafts with a legacy of heavy metals and acidic contamination in a pristine ecosystem now recognised as Great Blue Mountain World Heritage Area. The forest is predominantly comprised of different species of *Eucalyptus* trees. In addition to the airborne survey, ground-based spectra of the tree leaves were collected along the two accessible heavy metal contaminated pathways. The stream networks in the area were classified and the geospatial patterns of vegetation health were analysed along the Tonalli River, a major water tributary flowing through the National Park. Despite the inflow of contaminated water from the near-

mine streams, the measured vegetation health indices along Tonalli River were found to remain unchanged. The responses of the vegetation health indices between the near-mine and away-mine streams were found similar. Based on the along-stream and inter-stream analysis of the spectral indices of vegetation health, no significant impact of the heavy metal pollution could be noticed. The results indicate the possibility of the vegetation having developed immunity towards the high levels of heavy metal pollution over a century of exposure.

Keywords Vegetation stress · Heavy metal pollution · Hyperspectral remote sensing · Abandoned mines

Introduction

Abnormal levels of heavy metal exposure are known to adversely affect the photosynthetic process, leading to heavy metal-induced stress in vegetation. High levels of heavy metal concentration in the soil can inhibit enzyme activity (Assche and Clijsters 1990), alter the physicochemical and biochemical processes (Nagajyoti et al. 2010) and may negatively influence the plant health, growth and biomass accumulation (Clevers et al. 2004). Mukhopadhyay and Maiti (2011) demonstrated that adsorption and absorption of heavy metals in leaves could be used as a reliable indicator of chemical, air and soil pollution.

Heavy metal-induced changes in physiological process and leaf chemistry, in turn, could cause significant variation in the natural spectral characteristics of

B. P. Banerjee · S. Raval (✉)
Australian Centre for Sustainable Mining Practices, School of Mining Engineering, University of New South Wales, Sydney, NSW 2052, Australia
e-mail: simit@unsw.edu.au

B. P. Banerjee · S. Raval · H. Zhai
School of Mining Engineering, University of New South Wales, Sydney, NSW 2052, Australia

P. J. Cullen
School of Chemical Engineering, University of New South Wales, Sydney, NSW 2052, Australia

vegetation. These changes mainly occur in the visible and near-infrared regions of the electromagnetic spectrum. Imaging spectroscopy has emerged as a promising tool for monitoring vegetation health and induced stress due to heavy metal pollution in remote and/or over wider areas. Reusen et al. (2003) evaluated 18 potential vegetation stress indices to estimate the heavy metal-induced stress on *Pinus sylvestris* L. using Compact Airborne Spectrographic Imager (CASI). The vegetation stress levels were then used to map the distribution of heavy metal pollution over a region affected by historical non-ferrous industrial activities in Maatheid, Belgium. Rosso et al. (2005) measured several growth and physiological parameters including shoot reflectance in *Salicornia virginica* and correlated the symptoms with the contamination levels. The spectral response was found to be sensitive to early stress levels due to cadmium (Cd) and the lightweight petroleum. Ren et al. (2008) studied the spectral response of paddy plants grown in controlled amounts of lead (Pb)-contaminated soil. The contamination process reduced the canopy chlorophyll content (CCC) and caused the canopy spectral reflectance to increase over the VNIR region. Spectral derivatives such as normalised spectral absorption depth (Dn) and shifting distance (DS) of red edge position (REPs) revealed the variations in Pb concentration for canopy leaves. Barry et al. (2008) investigated defoliation and discolouration on two Australian *Eucalyptus* species (*E. globulus* and *E. pilularis*) using a set of 15 reflectance vegetation indices. Li et al. (2015) proposed a hyperspectral index to monitor the subtle changes in CCC of rice due to arsenic stress. The proposed index was reported to perform better than the random forest model and other indices.

Abandoned mine sites often leave a legacy of soil contamination, making it necessary to study such cases for guidance on protection and future mitigation strategies (Kostarelos et al. 2015). The town of Yerranderie in New South Wales, Australia, had several silver-lead-zinc mines that were abandoned since the late 1920s. In a previous study, Harrison et al. (2003) used core and surface sediment samples as well as samples from the surface watercourses to evaluate the distribution of lead (Pb), arsenic (As), zinc (Zn), copper (Cu), cadmium (Cd), mercury (Hg) and silver (Ag). The study reported that the metal concentrations at some places were up to 400 times higher than the ANZECC (Australian and New Zealand Environment and Conservation Council) and ARMCANZ (Agriculture and Resource Management Council of Australia and New

Zealand) guideline thresholds. Wright (2005) found 80 times higher levels of zinc above background in some parts of the Grose River where runoff occurs from areas surrounding the zinc-rich coalmine (canyon coalmine). Archer and Caldwell (2004) studied the response of six native species to metal contamination surrounding a silver mine in Yerranderie, i.e. common rush (*Juncus usitatus*), spiny headed mat rush (*Lomandra longifolia*), couch (*Cynodon dactylon*), bracken fern (*Pteridium esculentum*), black wattle (*Acacia decurrens*) and tea tree (*Melaleuca alternifolia*). Although different species were reported to exhibit variable proportion of accumulation of different metals, interestingly, *C. dactylon*, *J. usitatus* and *P. esculentum* displayed tolerance to high Cd concentrations while *C. dactylon*, *J. usitatus*, *M. alternifolia* and *L. longifolia* tolerated significantly higher Pb concentrations than the other species. Shamsoddini et al. (2014) employed ground-based spectroscopy to analyse metal contamination in the soil around some of the silver-zinc mine shafts located in this area. The study results exhibited higher accuracy for estimating As and Pb compared to other heavy metals through the spectral characteristics of the soil, while the approach failed for Ag.

Studies, to date, in this area have been based on ground-based point sampling method to investigate the contamination level in water (Wright 2005), soil (Harrison et al. 2003; Shamsoddini et al. 2014) and vegetation (Archer and Caldwell 2004). All precedent studies on this important region have confirmed the presences of excessive heavy metal in soil, water and vegetation; further studies are required to understand the effect of heavy metal on the local ecosystem and the distribution of heavy metal contamination at a larger spatial extent. However, the ground-based studies have been impeded by the difficult terrain and thick vegetation. By using airborne hyperspectral imaging technique for the first time, this study aims to assess the variability of vegetation health conditions as a response to contaminated water intake. Moreover, study of this area (Yerranderie) is significant for its rich history of mining and being a part of a United Nations Educational, Scientific and Cultural Organization (UNESCO) recognised world heritage site. Besides, the primary runoff in this area, Tonalli River, is the one of the major tributaries of Lake Burragarang which supplies approximately 80% of the potable water for the Greater Sydney region (Harrison et al. 2003; Shamsoddini et al. 2014). The investigation and monitoring of Yerranderie's water, land and vegetation does not only affect the preservation of local environments but also the well-beings of five million people that inhabit

the Greater Sydney Region. Furthermore, the significance is not limited to this specific area—although a global estimate of abandoned mines is absent, Australia alone has more than 50,000 abandoned mines (Unger et al. 2012). These sites are potential source of heavy metal pollution and the employed remote sensing methodology is more suitable compared to ground-based sampling techniques to monitor such areas on large spatial scales.

Materials and methods

This section details the datasets used and process workflow undertaken in this study. This includes description of the study area, field campaign to collect different in situ data (soil sampling and spectral measurements), source of ancillary information (contour data as geospatial layers), airborne camping undertaken to collect the hyperspectral data (sensor characteristics, configuration and flight details), radiometric correction and mosaic procedures, vegetation mask preparation, generation of vegetation indices, creation of stream buffer, and along and inter-stream analysis of the vegetation (Fig. 1).

Study site description

The study was performed over the forested landscape in Yerranderie, located 65 km southwest of Sydney in the

Blue Mountains National Park, New South Wales (NSW), Australia (34° 7' 9.25" S, 150° 30' 8.20" E coordinate and 640 m msl altitude). The area was historically mined for silver, lead and zinc mines which have been abandoned since the late 1920s. The location of ten such abandoned mine shafts is shown in Fig. 2 as yellow-coloured triangles.

The Tonalli River (Fig. 2) flowing diagonally from a southwest to northeast direction over the area is a tributary of Lake Burragorang that supplies 80% of the drinking water for the Sydney Region (Harrison et al. 2003; Shamsoddini et al. 2014). The forest cover, under primary investigation in this study, consists of different varieties of *Eucalyptus* tree species such as white strim bark, grey gum, red gum and iron bark.

Soil sampling and spectral measurements

A field campaign was performed along two down streams (N1 and N2 in Fig. 2) running from the abandoned Silver Peak (M6) and Colon Peak (M7) mineshafts. On-site spectral measurements of 53 bare ground and 51 vegetation leaf sample spectra were collected using a hand-held spectroradiometer (ASD Fieldspec Pro 3). In addition, the location coordinates of the sampling points were acquired using a differential global positioning system—DGPS (OmniSTAR HP).

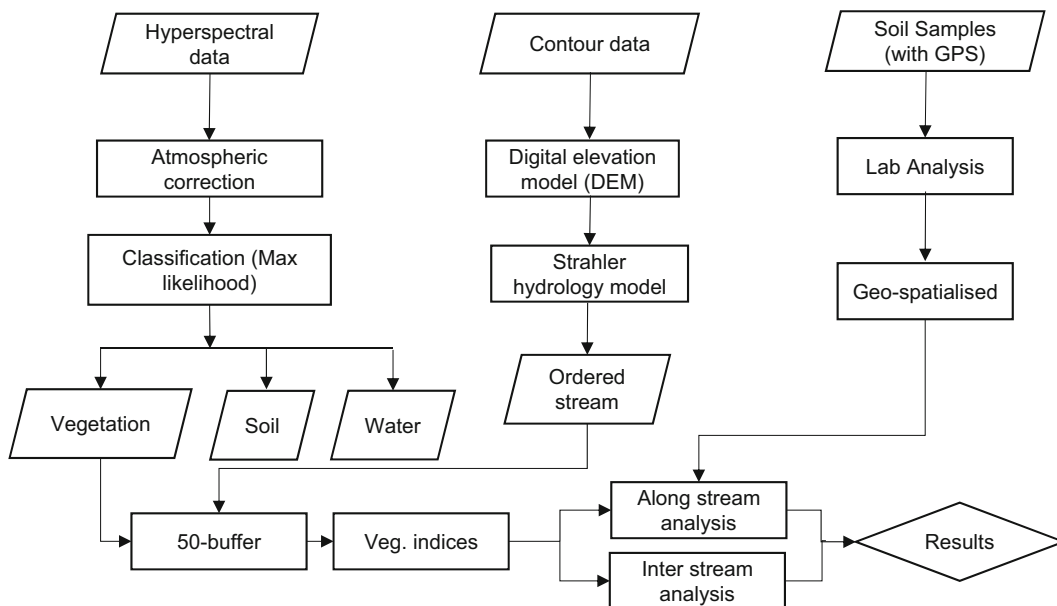


Fig. 1 Data and process workflow

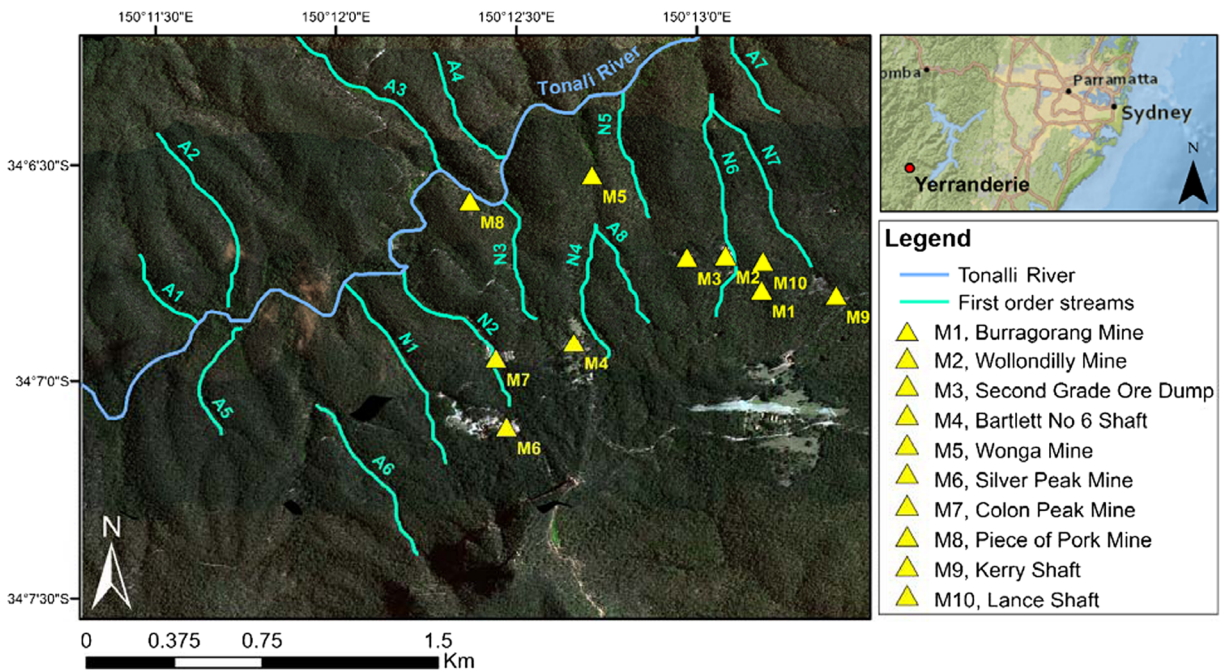


Fig. 2 The study area indicating mine sites (M1–M10), Tonalli River and its tributaries divided into two groups near mines (N1–N7) and away from the mine sites (A1–A7)

Geospatial layers

A 10-m spaced topographic contour data was acquired in digital format from Land and Property Information, NSW (LPI 2015). The location of underground mines was obtained from a Historic Yerranderie Town Map provided by NSW National Park (NSWNP 2015) and geospatialized in ArcGIS™.

Airborne campaign

Airborne hyperspectral datasets were acquired over this area using an on-board pushbroom-type HySpex VNIR 1600 sensor. The sensor was configured in the spectral mode of 160 wavelength bands over 400–1000 nm at 3.7 nm spectral and 12 bit radiometric resolution. Configured with a fore-optics of 17 degree field of view (FOV), the VNIR hyperspectral datasets were acquired at approximately 0.5 m ground resolution over approximately 0.6 km of the swath. The datasets were available as level 2 (L2)-processed ortho-rectified products in World Geodetic System (WGS84) datum and Universal Transverse Mercator (UTM) projection system. In total, 13 image strips ranging between 10 and 12 km in length were collected over the area. The flight was conducted between 9:55 am

and 10:55 am AEST covering the abandoned mine sites around Yerranderie and the surrounding vegetation cover.

Pre-processing—radiometric correction and mosaic

Out of the total 13 image strips, eight image strips were selected, based on the required subset coverage of 11.5 km × 7 km area around Yerranderie (Fig. 2). The selected strips were radiometrically corrected for atmospheric noise and converted to true reflectance using Fast Line-of-sight Atmospheric Analysis of Spectral Hypercubes (FLAASH) based on MODTRAN4 model (FLAASH 2009; FLAASH 2016) available in the image analysis software (ENVI™ 4.8). FLAASH uses the following radiometric model for spectral radiance at a sensor pixel, L in VNIR wavelengths over flat and Lambertian surfaces.

$$L = \left(\frac{A\rho}{1-\rho_e S} \right) + \left(\frac{B\rho_e}{1-\rho_e S} \right) + L_a \quad (1)$$

where ρ is the pixel surface reflectance, ρ_e is an average surface reflectance for the pixel and a surrounding region, S is the spherical albedo of the atmosphere, L_a is the radiance back scattered by the atmosphere, and A and B are coefficients for atmospheric and geometric conditions.

The values of A , B , S and L_a were determined from MODTRAN calculations that using the nadir viewing sensor orientations. The atmospheric model based on *Sub-Arctic Summer* (SAS), *rural-type* aerosol settings with visibility factor of 40 km, solar angles calculated from date and time of data acquisition, and mean surface elevation (640 m from msl) were selected for the MODTRAN calculation.

The corrected set of stripes was then mosaicked together with a 15-pixel feathering distance and colour balancing of overlapping adjacent stripes to remove radiometric abnormalities between the stripes (ENVI-Mosaicking 2013). The resultant reflectance spectra of the vegetation obtained through the airborne campaign were verified against the respective spectra of the collected vegetation samples using ASD Fieldspec (Fig. 3). The radiometrically corrected mosaicked product was deemed suitable for further analysis.

The spectral plot in Fig. 3 shows the comparison of leaf reflectance spectra of a single reference location obtained from the ground-based spectrometer and vegetation canopy reflectance spectra of the respective pixel acquired from the airborne imaging. A similar trend of both the reflectance curves is an indicative of proper radiometric correction performed by the MODTRAN model in the removal of atmospheric effects of the airborne data. The selected wavelength bands are shown with the vertical red lines in Fig. 3.

Vegetation mask

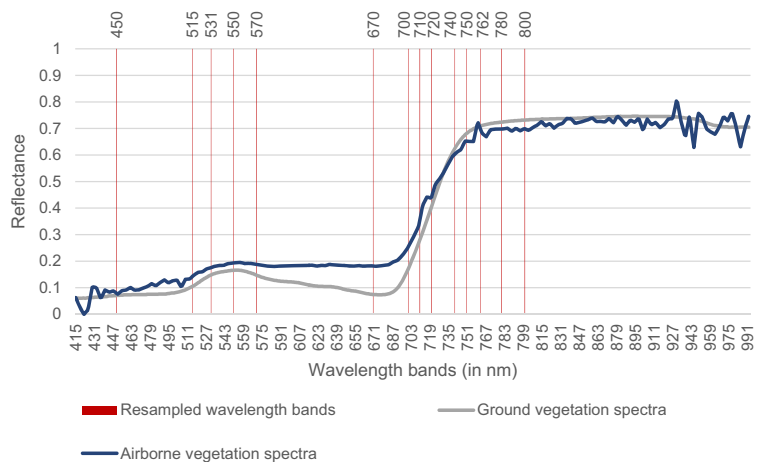
A supervised maximum likelihood classification (Richards and Richards 1999) in ENVI™ 4.8 was used

to classify the image into three major classes, i.e. bare ground, vegetation and water.

To compensate for the geometric inaccuracies of the hyperspectral data and dilution of precision (DOP) of the hand-held DGPS sensor measurements around the high *Eucalyptus* canopies, a 5 m × 5 m bounding box was created around individual sampling points and the pixels were treated as pure (homogeneous class) ground truth samples. With the hyperspectral data available at a spatial resolution of 0.5 m, a single bounding box equates to 100 pixels. Thus, a total of 5300 bare ground and 5100 vegetation ground truth pixels were obtained around the 53 bare ground and 51 vegetation sampling locations, respectively. In addition, another set of 5300 bare ground and 5100 vegetation pixels were visually identified using a combination of wavelength bands—455, 560 and 610 nm from the high-resolution hyperspectral data, covering the entire scene to justify a balanced sampling approach (Wei and Dunbrack 2013). The Tonalli River flows as a narrow stream, densely covered by the adjacent vegetation (tree canopies), and had a low water level during the period of the airborne campaign, as such pure water pixels are unable to be identified in the river. Instead, a total of 1000 sample water pixels were selected from a small water dam within the spatial extent of the hyperspectral image. The ‘field-derived’ and ‘image-identified’ samples were mixed and half of the total samples per class were randomly selected for supervised classification and the remainder used for accuracy assessment.

The performed classification achieved a classification accuracy of 99.38% for vegetation, 98.35% for soil and 94.86% for water. All 160 bands were used in the classification process. The classified vegetation class

Fig. 3 Comparison of ground-based leaf reflectance spectral measurement and airborne vegetation canopy reflectance spectra



was used as a spatial mask for the vegetation condition analysis. The process of vegetation masking excluded the soil and water pixels being incorrectly treated for vegetation condition assessment, thus eliminating any unanticipated source of error in the analysis stage. The output, vegetation class was used as a vegetation mask for the radiometrically corrected and mosaicked hyperspectral product for further analysis.

Vegetation indices

Pure vegetation-masked spectra from the airborne hyperspectral imagery (160 spectral bands) were spectrally downsampled and resampled to a set of 14 spectral bands, i.e. 450, 515, 531, 550, 570, 670, 700, 710, 720, 740, 750, 762, 780, and 800 nm. These 14 spectral bands were then used to produce hyperspectral vegetation indices related to chlorophyll, xanthophyll, blue/green ratio and canopy structures which are closely related to vegetation health. A list of vegetation indices used in this study are provided in Table 1. A set of 15 reflectance indices related to vegetation health have been earlier used for studying different species of *Eucalyptus* (Barry et al. 2008). It was recommended to use

multiple reflectance indices since no individual indices were found robust for all the different types of stress and on the different species. The selection of resources of indices (Table 1) in this study was improved upon this recommendation to obtain a comprehensive validation of the results in this study.

Digital elevation model and stream buffer creation

The measurements from the digital contour map were interpolated to produce a 1-m resolution digital elevation model (DEM) for the area in ArcGIS™. The DEM was further processed using the hydrology toolbox to create the stream network map of the area as per Strahler stream classification scheme. In this scheme, waterways are given an order according to the number of additional tributaries associated with each waterway (Strahler 1952). First-order streams are the lowest level of the permeant watercourses before they merge into the second-order stream, i.e. the Tonalli River.

The vegetation stress analysis due to heavy metals was focused around a 50-m buffer zone along the first-order streams. In this regard, the first-order streams were considered to be comprised of similar kind of

Table 1 List of vegetation indices employed in this study

Indices	Equation	Reference
Related to chlorophyll levels		
Vogelmann (VOG)	$VOG = R_{740}/R_{720}$	(Vogelmann et al. 1993)
Red edge (RE)	$RE = R_{750}/R_{710}$	(Zarco-Tejada et al. 2001)
TCARI	$TCARI = 3 \times \left[(R_{700} - R_{670}) - 0.2 \times (R_{700} - R_{550}) \times \left(\frac{R_{700}}{R_{670}} \right) \right]$	(Haboudane et al. 2002)
TCARI/OSAVI	$\frac{TCARI}{OSAVI} = \frac{TCARI}{\left[(1 + 0.16) \times \frac{R_{800} - R_{670}}{R_{800} - R_{670} + 0.16} \right]}$	(Haboudane et al. 2002)
MCARI2	$MCARI2 = 1.2 \times \frac{[1.2 \times (R_{800} - R_{550}) - 2.5 \times (R_{670} - R_{550})]}{(2 \times R_{800} + 1)^2 - (6 \times R_{800} - 5 \times \sqrt{R_{670}}) - 0.5}$	(Haboudane et al. 2004)
Related to xanthophyll levels		
PRI ₅₇₀	$PRI_{570} = \frac{R_{570} - R_{531}}{R_{570} + R_{531}}$	(Gamon et al. 1992)
PRI ₅₁₅	$PRI_{515} = \frac{R_{515} - R_{531}}{R_{515} + R_{531}}$	(Hernández-Clemente et al. 2011)
Blue/green ratios		
G	$G = \frac{R_{550}}{R_{670}}$	(Zarco-Tejada et al. 2005)
BGI2	$BGI2 = \frac{R_{450}}{R_{550}}$	(Zarco-Tejada et al. 2005)
Related to canopy structure		
NDVI	$NDVI = \frac{R_{800} - R_{670}}{R_{800} + R_{670}}$	(Rouse et al. 1974)
RDVI	$RDVI = \frac{R_{800} - R_{670}}{\sqrt{R_{800} + R_{670}}}$	(Roujean and Breon 1995)
TVI	$TVI = 0.5 \times [120 \times (R_{750} - R_{550}) - 200 \times (R_{670} - R_{550})]$	(Broge and Leblanc 2001)
MTVI1	$MTVI1 = 1.2 \times [1.2 \times (R_{800} - R_{550}) - 2.5 \times (R_{670} - R_{550})]$	(Haboudane et al. 2004)

vegetation. Furthermore, the vegetation along the first-order streams is more likely to receive a similar amount of water year-round, thereby normalising to some degree the effects of water stress on reflectance spectra of vegetation.

Along-stream vegetation analysis

To analyse the variation of vegetation health along the Tonalli River, the vegetation indices' values within a search radius of 50 m were averaged every 10 m along the length of the Tonalli River. A lengthwise profile of vegetation health along the Tonalli River was used to analyse the variation.

Inter-stream vegetation analysis

The inter-stream vegetation condition assessment was targeted to examine the spatial abundance of healthy/unhealthy (high/low vegetation index value) pixels within streams near potential heavy metal contaminations against the streams free from sources of pollution. Streams near abandoned mines were labelled as near (N1–N7) to mine streams and others as away (A1–A7) to mine streams (Fig. 2). To analyse the inter-stream vegetation condition, a superimposed histogram approach has been used. A histogram naturally creates a plot of frequency measures of a variable over quantised bins. The reported frequency in the histogram was used as an indication of the spatial abundance of healthy/unhealthy (high/low vegetation index value) pixels. All the near (N1–N7) and away (A1–A7) from the mines stream histograms were then

superimposed. Interpretation of the superimposed histogram is visually simple and has been conceptualised in Fig. 4. Conceptually, the frequency distribution of near mine (N) and away from mine (A) streams should be similar and should almost overlap each other, when both the streams are surrounded by the vegetation of similar health conditions. On the other hand, if the vegetation in the near mine streams is affected by pollution then the frequency distributions should be skewed opposite to each other, i.e. N towards the lesser vegetation index values and A towards higher vegetation index values. The relationship will invert when the vegetation index values are inversely proportional to the health parameters, as in the case of PRI₅₇₀ and PRI₅₁₅.

Results and discussion

Along-stream vegetation analysis

Figure 5 plots the variation of vegetation indices' values along the flow path of the Tonalli River, which is the major river in the study area. Linear values of all the indices were plotted on the primary Y-axis except the value of TVI, which was scaled logarithmically and plotted on secondary Y-axis since the data range of TVI was disproportionate from the range of the rest indices. During periods of heavy rainfall, metal contaminants from the nearby derelict mines in Yerranderie are transported to the Tonalli River and, from there, to Lake Burrangorang (Wright 2005). The objective of the along-stream analysis on the vegetation along the Tonalli River

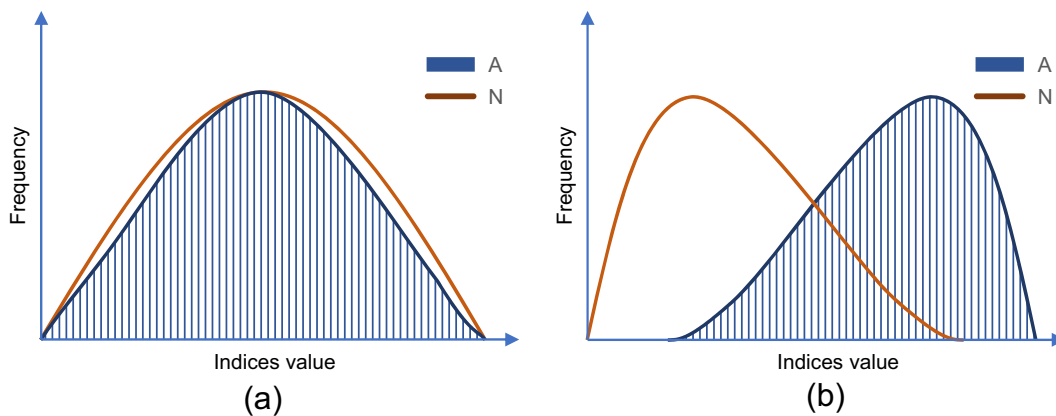


Fig. 4 Conceptual representation of superimposed histograms for scenarios **a** both near to mine (N) and away from mine (A) streams have similar spatial abundance of healthy/unhealthy pixels, and **b**

near to mine (N) streams have lower spatial abundance of healthy pixels and away from mine (A) streams have higher spatial abundance of healthy pixels

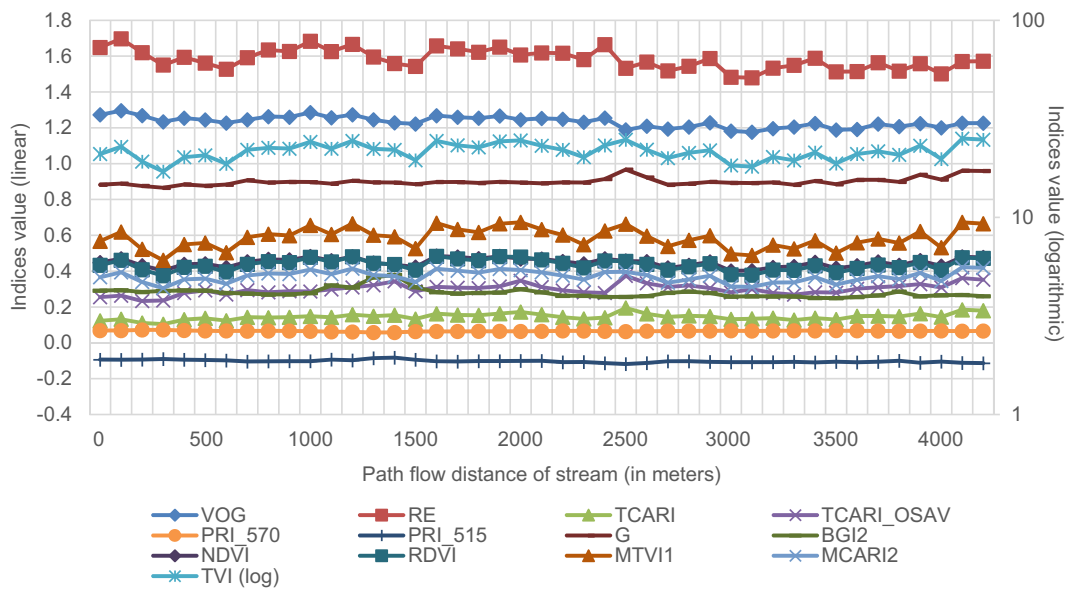


Fig. 5 Variation (linear and logarithmic) of vegetation indices' values along the Tonalli River

was to identify any variation in the vegetation reflectance properties because of the prevalent heavy metal pollution. Spectroscopic reflectance indices of the vegetation generally exhibit a decreasing tendency (relationship is inverted for PRI_{570} and PRI_{515}) in response to stress. However, all the plots in Fig. 5 show only a minor variation of the indices' values related to chlorophyll, xanthophyll, blue/green ratio and canopy structures along the flow path direction. Moreover, there was no major drop in the vegetation indices response where the first-order tributary streams from the abandoned mines (N1–N7) join the Tonalli River and beyond. Tolerance to acidic soil and contamination from Pb and Cd has been previously reported on few phytostabilisation plant species present in the study area (Archer and Caldwell 2004). The fact that all the indices related to bio-physiochemical parameters point to no significant variation in the gross forest health despite the presence of high level of contamination supports the conclusion that the hyperspectral analysis shows no major impact of heavy metal contamination on the vegetation of the studied area and leads the possibility that the vegetation might have developed resilience against the level of contamination in the area.

Inter-stream vegetation analysis

Figure 6 shows an inter-comparison of vegetation condition around first-order streams with a nearby

abandoned mine in its path (N1–N7) or away from abandoned mine (A1–A8) contaminations using the conceptualised superimposed histogram method. According to the method, the frequency distribution curves of near to mine (N1–N7) and away from mine (A1–A8) streams should overlap each other, when vegetation around both the streams is of similar health conditions. However, if the vegetation in the near to mine streams (N1–N7) is affected by pollution then corresponding frequency distribution curves will not overlap. Instead, the peak values of the frequency distribution curves around near to mine streams (N1–N7) should be significantly lower than that of away from mine streams (A1–A8). This behaviour would be invert when the vegetation index values are inversely proportional to the health parameters (PRI_{570} and PRI_{515}). In this analysis, the superimposed histograms of the different vegetation indices generated for (N1–N7) and (A1–A8) found to overlap each other in variably for each vegetation indices (Fig. 6). This strongly suggests that the vegetation condition was similar for both the mining and non-mining streams, more particularly the percentage of vegetation cover with healthy spectral response was identical. Similar to the along-stream analysis, the inter-stream analysis of the vegetation indices related to chlorophyll, xanthophyll, blue/green ratio and canopy structures supports a similar conclusion. Although a contrast of the vegetation indices' values was likely between the contaminated streams (near to the mine

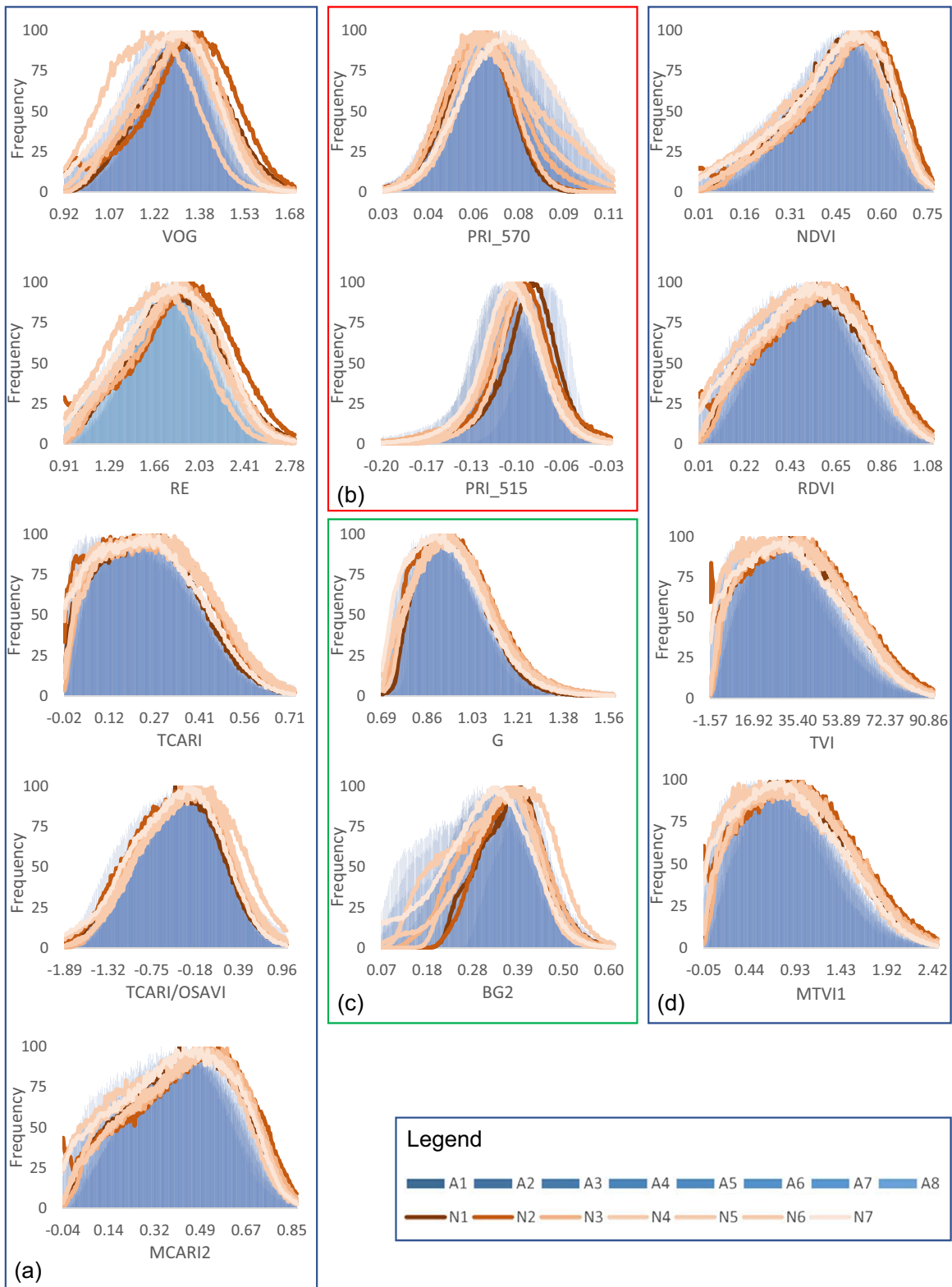


Fig. 6 Superimposed histograms showing the spatial abundance of healthy/unhealthy pixels based on **a** chlorophyll, **b** xanthophyll, **c** blue/green ratio and **d** canopy structure

shafts) and un-contaminated streams (away from the mine shafts), the observation was not unaccountable since other species (*C. dactylon*, *J. usitatus* and *L. longifolia*), resilient against heavy metal contaminations, have been previously identified in this region (Archer and Caldwell 2004).

Conclusions

In this study, the health condition of vegetation exposed to heavy metal pollution was assessed at a very high spatial extent and resolution around Yerranderie's derelict mining area using airborne hyperspectral data in this study. The method is identified as a useful tool to monitor vegetation condition on a larger spatial extent, although more understanding of the spectral response *Eucalyptus* trees to heavy metal stress needs to be obtained.

This study adopted a systematic approach to first radiometrically correct and analyse the hyperspectral data. Then a set of 13 different vegetation indices related to different bio-physiochemical parameters (chlorophyll, xanthophyll, blue/green/red ratio and structure) were derived over the VNIR (400–1000 nm) portion of the electromagnetic spectrum. The selected indices indicated natural levels of values in the region. Future spectroscopic analysis therefore could employ SWIR (1000–2500 nm) region of electromagnetic spectrum to identify possible variation of reflectance properties due to the heavy metal stress.

A superimposed histogram method was proposed to visualise vegetation indices data from around multiple contaminated and un-contaminated streams. The method simplifies the comparative interpretation of the vegetation health status through use of frequency distribution curves of vegetation indices. Furthermore, the technique retains information for each pixel in a zone (N1–N7 or A1–A7) in the corresponding frequency distribution curve, which is lost when using statistical mean or median value for the entire zone instead. Therefore, the method could also be used as a lossless inter-comparative visualisation tool in other scenarios as well.

Along-stream analysis for the Tonalli River and inter-stream analysis for the first-order tributaries was restricted to a buffer distance zone of 50 m. Vegetation in these buffer zones is more likely to comprise of similar type of *Eucalyptus* species. Therefore, the approach is suitable to evaluate stress in vegetation due to heavy metal by eliminating bias from secondary sources.

The along-stream analysis indicated no major decline of the vegetation profile along the Tonalli River despite the inflow of water contaminated with heavy metals through first-order tributary streams from the abandoned mines (N1–N7). The inter-stream comparison of the vegetation indices revealed similar response of vegetation in streams near and away from the abandoned mine locations. Our observation through airborne spectroscopy on tree-type forest vegetation cover is therefore in line with the results of Archer and Caldwell (2004) with understorey plant species. Their report identified few potential phytostabilisation plant species (*C. dactylon*, *J. usitatus* and *L. longifolia*), due to tolerance of acid soils and tolerance and/or accumulation of significantly higher concentrations of Pb and Cd. It is therefore highly likely that, 97 years after the mining activity has ceased in this area, local vegetation may have developed sufficient resistance and adapted to the heavy metals.

Acknowledgements We thank Dr. Ali Shamsoddini and Shiyun Yu for their precedent survey of soil sampling and collection of ground vegetation spectra at Yerranderie.

Funding information This independent research was funded by the Australian Centre for Sustainable Mining Practices (ACSMP), School of Mining Engineering, UNSW, Australia, as a Ph.D. scholarship for the first author. UNSW is also thanked for providing Taste of Research (TOR) scholarship for the third author.

Compliance with ethical standards

Conflict of interest The authors declare that they have no conflict of interest.

References

- Archer, M., & Caldwell, R. (2004). Response of six Australian plant species to heavy metal contamination at an abandoned mine site. *Water, Air, and Soil Pollution*, 157(1–4), 257–267.
- Assche, F. V., & Clijsters, H. (1990). Effects of metals on enzyme activity in plants. *Plant, Cell & Environment*, 13(3), 195–206.
- Barry, K. M., Stone, C., & Mohammed, C. L. (2008). Crown-scale evaluation of spectral indices for defoliated and discoloured eucalypts. *International Journal of Remote Sensing*, 29(1), 47–69. <https://doi.org/10.1080/01431160701281056>.
- Broge, N. H., & Leblanc, E. (2001). Comparing prediction power and stability of broadband and hyperspectral vegetation indices for estimation of green leaf area index and canopy chlorophyll density. *Remote Sensing of Environment*, 76(2), 156–172.

- Clevers, J. G. P. W., Kooistra, L., & Salas, E. A. L. (2004). Study of heavy metal contamination in river floodplains using the red-edge position in spectroscopic data. *International Journal of Remote Sensing*, 25(19), 3883–3895. <https://doi.org/10.1080/01431160310001654473>.
- ENVI-Mosaicking. (2013). *ENVI classic tutorial: mosaicking*. Boulder: Exelis Visual Information Solutions Inc..
- FLAASH. (2009). *Atmospheric correction module: QUAC and Flaash user guide v. 4.7*. Boulder: ITT Visual Information Solutions Inc..
- FLAASH. (2016). FLAASH background. Harris Geospatial Solutions. <http://www.harrisgeospatial.com/docs/BackgroundFLAASH.html>. Accessed 18/10/2016 2016.
- Gamon, J. A., Peñuelas, J., & Field, C. B. (1992). A narrow-waveband spectral index that tracks diurnal changes in photosynthetic efficiency. *Remote Sensing of Environment*, 41(1), 35–44. [https://doi.org/10.1016/0034-4257\(92\)90059-S](https://doi.org/10.1016/0034-4257(92)90059-S).
- Haboudane, D., Miller, J. R., Tremblay, N., Zarco-Tejada, P. J., & Dextraze, L. (2002). Integrated narrow-band vegetation indices for prediction of crop chlorophyll content for application to precision agriculture. *Remote Sensing of Environment*, 81(2), 416–426.
- Haboudane, D., Miller, J. R., Pattey, E., Zarco-Tejada, P. J., & Strachan, I. B. (2004). Hyperspectral vegetation indices and novel algorithms for predicting green LAI of crop canopies: modeling and validation in the context of precision agriculture. *Remote Sensing of Environment*, 90(3), 337–352. <https://doi.org/10.1016/j.rse.2003.12.013>.
- Harrison, J., Heijnis, H., & Caprarelli, G. (2003). Historical pollution variability from abandoned mine sites, Greater Blue Mountains World Heritage Area, New South Wales, Australia. *Environmental Geology*, 43(6), 680–687. <https://doi.org/10.1007/s00254-002-0687-8>.
- Hernández-Clemente, R., Navarro-Cerrillo, R. M., Suárez, L., Morales, F., & Zarco-Tejada, P. J. (2011). Assessing structural effects on PRI for stress detection in conifer forests. *Remote Sensing of Environment*, 115(9), 2360–2375. <https://doi.org/10.1016/j.rse.2011.04.036>.
- Kostarelos, K., Gavriel, I., Stylianou, M., Zissimos, A. M., Morisseau, E., & Dermatas, D. (2015). Legacy soil contamination at abandoned mine sites: making a case for guidance on soil protection. *Bulletin of Environmental Contamination and Toxicology*, 94(3), 269–274. <https://doi.org/10.1007/s00128-015-1461-4>.
- Li, X., Liu, X., Liu, M., Wang, C., & Xia, X. (2015). A hyperspectral index sensitive to subtle changes in the canopy chlorophyll content under arsenic stress. *International Journal of Applied Earth Observation and Geoinformation*, 36, 41–53. <https://doi.org/10.1016/j.jag.2014.10.017>.
- LPI. (2015). Land and property information: topographic map of Wollondilly. <http://www.lpi.nsw.gov.au>. Accessed 25/01/2015 2015.
- Mukhopadhyay, S., & Maiti, S. K. (2011). Trace metal accumulation and natural mycorrhizal colonisation in an afforested coalmine overburden dump: a case study from India. *International Journal of Mining, Reclamation and Environment*, 25(2), 187–207. <https://doi.org/10.1080/17480930.2010.548663>.
- Nagajyoti, P. C., Lee, K. D., & Sreekanth, T. V. M. (2010). Heavy metals, occurrence and toxicity for plants: a review. *Environmental Chemistry Letters*, 8(3), 199–216. <https://doi.org/10.1007/s10311-010-0297-8>.
- NSWNP. (2015). New South Wales National Park: Historic Yerranderie Township. <http://www.yerranderie.com>. Accessed 25/01/2015 2015.
- Ren, H., Zhuang, D., Pan, J., Shi, X., & Wang, H. (2008). Hyperspectral remote sensing to monitor vegetation stress. *Journal of Soils and Sediments*, 8(5), 323. <https://doi.org/10.1007/s11368-008-0030-4>.
- Reusen, I., Bertels, L., Debacker, S., Debruyne, W., Scheunders, P., & Sterckx, S. (2003). Detection of stressed vegetation for mapping heavy metal polluted soil. In 3rd EARSeL Workshop on Imaging Spectroscopy, 2003 (pp. 13–16).
- Richards, J. A., & Richards, J. (1999). Remote sensing digital image analysis (Vol. 3): Springer.
- Rosso, P. H., Pushnik, J. C., Lay, M., & Ustin, S. L. (2005). Reflectance properties and physiological responses of *Salicornia virginica* to heavy metal and petroleum contamination. *Environmental Pollution*, 137(2), 241–252. <https://doi.org/10.1016/j.envpol.2005.02.025>.
- Roujean, J., & Breon, F. (1995). Estimating PAR absorbed by vegetation from bidirectional reflectance measurements. *Remote Sensing of Environment*, 51(3), 375–384. [https://doi.org/10.1016/0034-4257\(94\)00114-3](https://doi.org/10.1016/0034-4257(94)00114-3).
- Rouse, J., Haas, R., Schell, J., Deering, D., & Harlan, J. (1974). *Monitoring the vernal advancement of retrogradation of natural vegetation (Type III, Final Report)* (p. 371). Greenbelt: NASA/GSFC.
- Shamsoddini, A., Raval, S., & Taplin, R. (2014). Spectroscopic analysis of soil metal contamination around a derelict mine site in the Blue Mountains, Australia. *ISPRS Annals of the Photogrammetry. Remote Sensing and Spatial Information Sciences*, 2(7), 75–79. <https://doi.org/10.5194/isprannals-II-7-75-2014>.
- Strahler, A. N. (1952). Hypsometric (area-altitude) analysis of erosional topography. *Geological Society of America Bulletin*, 63(11), 1117–1142.
- Unger, C., Lechner, A., Glenn, V., Edraki, M., & Mulligan, D. (2012). Mapping and prioritising rehabilitation of abandoned mines in Australia. Proceedings of the Life of Mine 2012, Maximising mine rehabilitation outcomes, AusIMM/CMLR, 2012.
- Vogelmann, J., Rock, B., & Moss, D. (1993). Red edge spectral measurements from sugar maple leaves. *Remote Sensing*, 14(8), 1563–1575.
- Wei, Q., & Dunbrack Jr., R. L. (2013). The role of balanced training and testing data sets for binary classifiers in bioinformatics. *PLoS One*, 8(7), e67863.
- Wright, I. A. (2005). *Australian freshwater midges (Chironomidae: Diptera)*. Australia: University of Western Sydney.
- Zarco-Tejada, P. J., Miller, J. R., Noland, T. L., Mohammed, G. H., & Sampson, P. H. (2001). Scaling-up and model inversion methods with narrowband optical indices for chlorophyll content estimation in closed forest canopies with hyperspectral data. *IEEE Transactions on Geoscience and Remote Sensing*, 39(7), 1491–1507. <https://doi.org/10.1109/36.934080>.
- Zarco-Tejada, P. J., Berjón, A., López-Lozano, R., Miller, J. R., Martín, P., Cachorro, V., González, M. R., & de Frutos, A. (2005). Assessing vineyard condition with hyperspectral indices: leaf and canopy reflectance simulation in a row-structured discontinuous canopy. *Remote Sensing of Environment*, 99(3), 271–287. <https://doi.org/10.1016/j.rse.2005.09.002>.